Influence of machine control strategy on electric vehicle range

Pierre Caillard, Frederic Gillon, Michel Hecquet, Noëlle Janiaud

To cite this version:

Pierre Caillard, Frederic Gillon, Michel Hecquet, Noëlle Janiaud. Influence of machine control strategy on electric vehicle range. EVER Conference On Ecological Vehicles and Renewable Energies, Apr 2014, Monaco, Monaco. hal-01730148

HAL Id: hal-01730148
https://hal.archives-ouvertes.fr/hal-01730148

Submitted on 13 Mar 2018

HAL is a multi-disciplinary open access archive for the deposit and dissemination of scientific research documents, whether they are published or not. The documents may come from teaching and research institutions in France or abroad, or from public or private research centers.

L'archive ouverte pluridisciplinaire **HAL**, est destinée au dépôt et à la diffusion de documents scientifiques de niveau recherche, publiés ou non, émanant des établissements d'enseignement et de recherche français ou étrangers, des laboratoires publics ou privés.

Influence of machine control strategy on electric vehicle range

Pierre CAILLARD[1], Frederic GILLON[1], Michel HECQUET[1], Noëlle JANIAUD[2]
[1]ECLille, L2EP, CS 20048 Villeneuve d'Ascq, France, pierre.caillard@ec-lille.fr
[2]Renault, Technocentre, 78288 Guyancourt, France

***Abstract*—An optimized control strategy for induction machines is presented and compared to classic strategies. The described method allows to optimize voltage and frequency for a steady state equivalent circuit model of three-phase induction machine. This method is applied to an electric vehicle by simulating driving cycles and calculating energy consumption. The potential gain for the optimized control strategy is discussed.**

Keywords—induction machine, control strategy, driving cycle, energy efficiency, optimization

I. INTRODUCTION

Electric vehicles (EV) are one of the solutions to solve local pollution issues. With the current technologies, their main limitation is a limited range compared to internal combustion engines. This range can be increased due to improved design of the electric powertrain, by relying on modeling and simulation tools in order to optimize the system [1]. Usually, the electric powertrain design starts with geometry sizing of each component [2]. The electric machine design can be defined with a direct sizing formulation [3], or with an optimization procedure to explore different possibilities [4]. To simplify this optimization, control strategy is usually not a priority and a basic control is set up; this strategy is studied in a latter design step [5][6]. This paper deals with the benefits of control strategy optimization on a model that will be adapted for optimal design process. The objective is to investigate the effect of the control strategy on the energy consumption of an electric vehicle during driving cycles. The proposed optimization strategy maximizes efficiency for each operating point in order to minimize overall energy consumption. The studied machine type is a three-phase induction machine modeled with an analytical steady state equivalent circuit taking into account iron losses and saturation [7]. The paper is organized as follows. Section II describes the machine model. The optimized control strategy is presented in section III. Finally a comparison between this strategy and a classic constant flux control strategy is discussed.

II. INDUCTION MACHINE MODEL

The studied machine is a 4 poles squirrel cage induction machine dedicated to an electric vehicle. The machine is modeled with a per phase equivalent circuit. This steady state analytical model has low computational time and enough accuracy for energy estimation on driving cycle [6][8].

A. Equivalent circuit

Notations:
V_1 : per-phase voltage (V)
V_{1max} : machine max available voltage (V)
E : electromotive force (V)
r_1 : stator resistance (Ω)
x_1 : stator leakage reactance (Ω)
r_2' : rotor resistance (Ω)
x_2' : rotor leakage reactance (Ω)
r_m : iron loss resistance (Ω)
x_m : magnetizing reactance (Ω)
l_i : inductance of part i; $i \in [1,2',m]$ (H)
l_{m0} : magnetizing inductance part depending only on the geometry (H)
l_{11} : stator slot leakage inductance (H)
l_{12} : head of winding inductance (H)
l_{13}: stator zig-zag inductance part depending only on the geometry (H)
s : slip
ω_s : stator pulse (rad/s)
Ω_r : rotor mechanical speed (rad/s)
f : stator frequency (Hz)
p : poles pair number
Ks : saturation coefficient
T : torque (Nm)

For a squirrel cage rotor, the equivalent circuit is the following [9]:

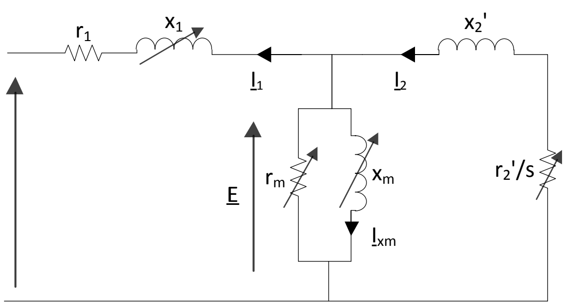

Fig. 1. Induction machine equivalent circuit

The reactance values x_i (x_1, x_2', x_m) depend on the stator frequency f through the relation:

$$x_i = l_i\, \omega_s = l_i\, 2\, \pi\, f \qquad (1)$$

The slip s is calculated as:

$$s = \frac{\omega_s - p\, \Omega_r}{\omega_s} \qquad (2)$$

The focus of this paper is the impact of the control strategy optimization, that's why the geometry will be fixed. If V_1 (respectively E), f, and Ω_r are known, the circuit can be solved (see [9]); the outputs are E (respectively V_1), torque, currents, losses, efficiency, power factor, and temperatures if a thermal model is added. Flux and currents are supposed to be ideal sin waves (1^{st} harmonic model). For a machine dedicated to electric vehicle with variable speed and torque, saturation and iron losses can't be neglected, and the voltages V_1 and E need to be calculated by solving the equivalent circuit.

B. Saturation

Saturation is taken into account in l_m and l_1 inductances, with a saturation coefficient Ks [10][11]:

$$l_m = \frac{l_{m0}}{Ks} \qquad (3)$$

$$l_1 = l_{11} + l_{12} + \frac{l_{13}}{Ks} \qquad (4)$$

The Ks coefficient is calculated as described in Fig. 2. Inductions are computed in different parts of the machine: air gap, stator tooth, stator yoke, rotor tooth, and rotor yoke. Fig. 2. is a flow chart summing up the calculations. A control strategy is needed to get the output torque equal to torque setpoint by finding the adequate E and f.

C. Iron losses

Iron losses P_{iron} are computed analytically, and depend on frequency and inductions in the different parts of the machine. They are divided into eddy current and hysteresis losses [12]. Then the iron loss resistance r_m is calculated by:

$$r_m = \frac{3 \times E^2}{P_{iron}} \qquad (5)$$

D. Validation

The model has been validated on a study case machine with experimental results. The following table gives the model error compared to the experiments:

TABLE I. COMPARISON MODEL AND EXPERIMENT IN %

Output	***Model error Operation point 1***	***Model error Operation point 2***
Torque	6%	7%
Total losses	7%	5%
Current	3%	4%

Operating point 1 is at low speed, middle torque, while point 2 is at high speed low torque. Other operating points have been validated with an error always under 10%.

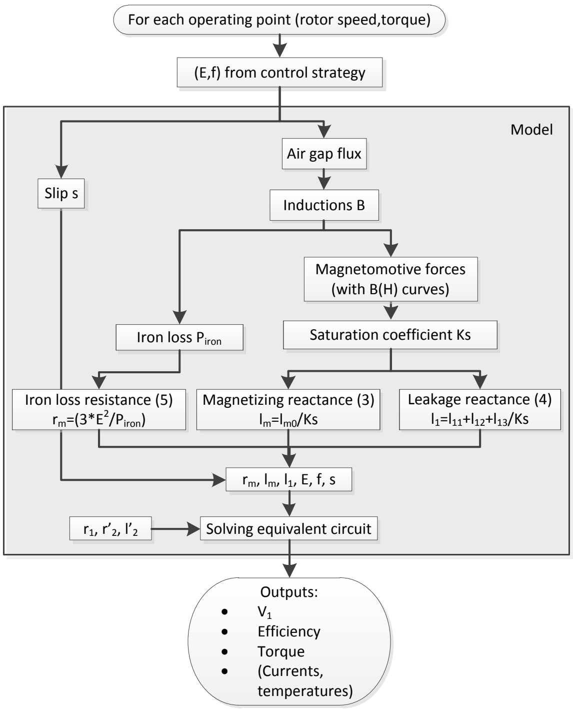

Fig. 2. Model flow chart

III. CONTROL STRATEGY OPTIMIZATION ALGORITM

Several pairs *(E,f)* can lead to the same operating point (rotor speed,torque) [8]. Choosing the best *(E,f)* in terms of efficiency or current represents the control strategy optimization in this work. A usual method to get these values is to keep the flux constant, which means keep the E/f ratio constant. But E can't be directly controlled, so a simplification is often made: V_1/f is kept constant [6]. This hypothesis is true if the voltage difference between V_1 and E is low. For better performances, these values can be optimized with different objectives such as minimizing current or maximizing efficiency in an optimization loop. These strategies also have to limit the machine voltage to a maximum threshold called V_{1max}. In this paper, three strategies will be compared: A) "$V_1/f=k_1$" / B) "$E/f=k_2$" / C). Optimization. k_1 and k_2 are two constants for operating points without field weakening.

A. "$V_1/f=k_1$" strategy

With the "$V_1/f=k_1$" strategy, the $k_1=V_1/f$ ratio is kept constant until V_1 reaches the maximum then k_1 has to decrease for field weakening. This k_1 is usually calculated at the nominal operating point [13]. Keeping this ratio constant generally goes with the hypothesis that resistance r_1 is low so E can be approximated with V_1 [10]. With this method, the required torque is not respected, especially for low speeds where r_1 can't be ignored. The following plot represents the torque error in % when considering $E=V_1$. Speed and torque are displayed per unit (p.u.):

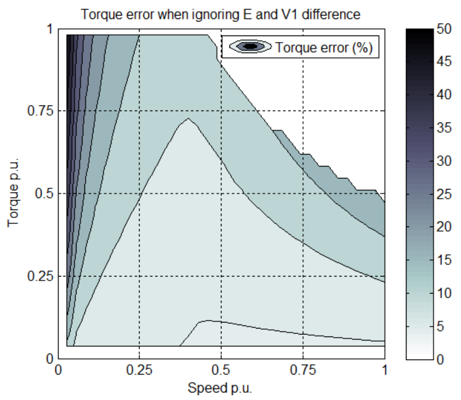

Fig. 3. Torque error in % when neglecting E and V1 difference

To solve this issue, an optimization algorithm has been used (detailed in part C. but with a different objective function):

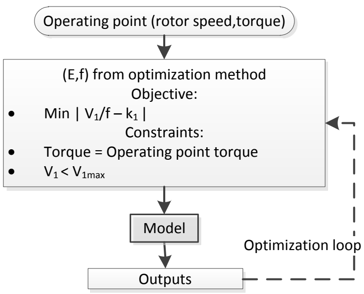

Fig. 4. Optimization method to get $V_1/f=k_1$

The objective is to minimize | $V_1/f - k_1$ | so that it's close to 0 as long as V_1 didn't reach V_{1max}, and torque is an equality constraint to get the required operating point torque. With this method, the difference between E and V_1 is not disregarded.

B. "$E/f=k_2$" strategy

With the "$E/f=k_2$" strategy, the $k_2=E/f$ ratio is kept constant, resulting in a constant flux. The constant k_2 ratio for $V_1<V_{1max}$ is called k_{2init}. This k_{2init} can be calculated at the nominal operating point. To get the required torque, the following torque equation is solved:

$$T = \frac{3\,p\,E^2}{\omega_s}\,\frac{\frac{r_2{'}}{s}}{\frac{r_2{'}^2}{s}+x_2'^2} = f(\Omega_r, k_2, f) = a\,f^2 + b\,f + c \qquad (6)$$

Where a, b and c are coefficients depending on Ω_r and k_2. For a specific operating point with a known k_2, the 2nd order following equation can be solved:

$$f = \frac{1}{4\,\pi\,T\,l'_2}\Big[3\,p\,k_2^2 r'_2 + 2\,T\,l_2'^2\,p\,\Omega_r - \sqrt{\left(3\,p\,k_2^2 r'_2 + 2\,T\,l_2'^2\,p\,\Omega_r\right)^2 - 4\,T\,l'_2\left(T\,r_2'^2 + T\,(l'_2\,p\,\Omega_r)^2 + 3\,p^2 k_2^2 r'_2\,\Omega_r\right)}\,\Big] \qquad (7)$$

Then E can be deduced:

$$E = f\,k_2 \qquad (8)$$

The following flow chart describes how the V_{1max} limit is respected:

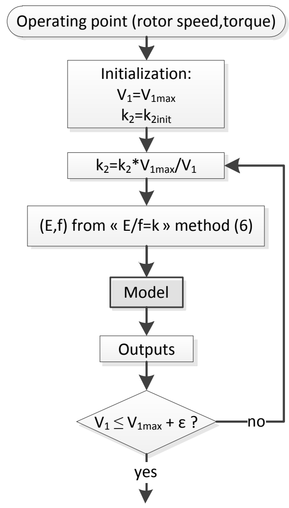

Fig. 5. "$E/f=k_2$" strategy flow chart

For high frequencies, the calculated V_1 is above V_{1max}. To get $V_1=V_{1max}$, the k_2 ratio is decreased by being multiplied by V_{1max} / V_1. That means that if the V_1 value is for example 20% too high, the k_2 ratio will be decreased by 20%. This method leads to $V_1=V_{1max}$ + ε (with ε a small error, typically 0.1% of V_{1max}) in very few iterations (3 max iterations with the example machine). This method has a very low computational time: ~0.5s for 500 operating points.

C. Optimization strategy

The optimization strategy consists in using an optimization algorithm to find the values for E and f that will maximize or minimize an objective. For maximizing range on a driving cycle, an objective can be to maximize powertrain (battery, inverter, motor) efficiency on each operating point. This study focuses on the machine so the chosen objective is to maximize efficiency η on each operating point. Required torque T_0 and voltage limit V_{1max} are handled as constraints.

$$\begin{aligned}
\underset{\mathbf{x}}{\text{Maximize}} \quad & \eta(\mathbf{x}) \\
\text{subject to} \quad & V_1(\mathbf{x}) - V_{1max} \le 0 \\
& T(\mathbf{x}) - T_0 = 0 \\
\text{with} \quad & \mathbf{x} = [E, f] \\
& 0 \le E \\
& f_{min} \le f
\end{aligned} \qquad (8)$$

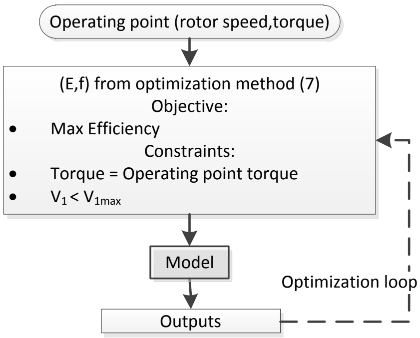

Fig. 6. Optimization strategy flow chart

In this paper, only operating points with positive torque are considered. Minimum frequency f_{min} corresponds to the rotor mechanical speed:

$$f_{min} = \frac{p\,\Omega_r}{2\pi} \tag{9}$$

Since slip frequency is always low, f is only a few Hertz more than f_{min}. The selected algorithm is sequential quadratic programming (SQP) with the fmincon MATLAB® function. This method is strongly recommended to handle constraints [14]. This method computational time is higher: ~40s for 500 operating points.

IV. Application on a Driving Cycle

Before calculating the energy consumption on driving cycles with a study case on a small vehicle, efficiency and power maps have been plotted to compare the 3 strategies.

A. *Speed/Torque maps*

The following figures represent the efficiency map for all speed and torque operating points. The maximum torque is limited by the maximum current available and the maximum power by the maximum voltage V_{1max}.

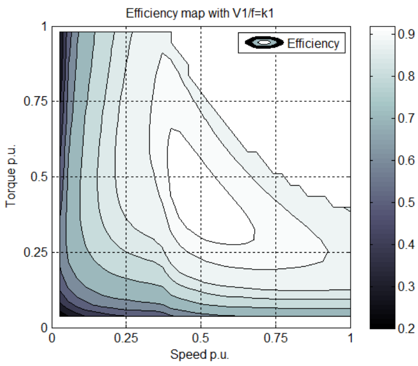

Fig. 7. Efficiency map with "$V_1/f=k_1$" strategy

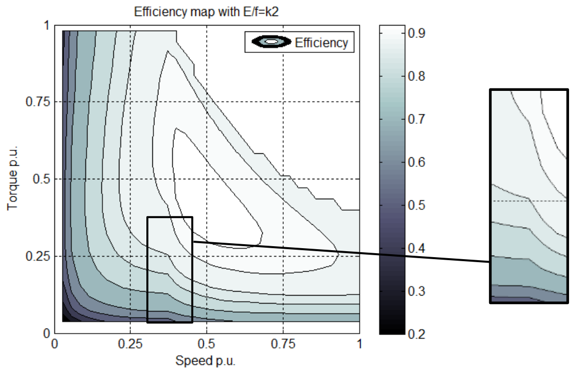

Fig. 8. Efficiency map with "$E/f=k_2$" strategy and focus at speed=0.325p.u

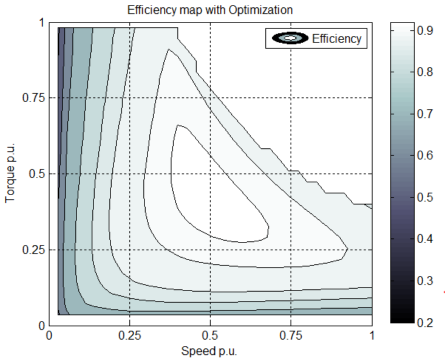

Fig. 9. Efficiency map with Optimization strategy

The behavior at approximately speed=0.325p.u. on Fig. 7. and 8. comes from the maximum voltage V_{1max} that have been reached. This can be observed by looking at the "*E/f*" ratio for a constant torque, e.g Torque=0.25 p.u.

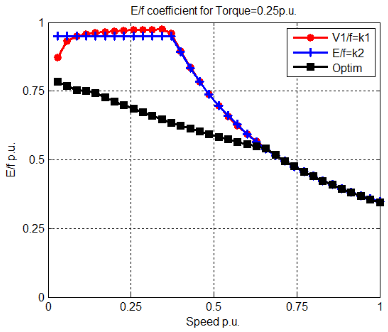

Fig. 10. "*E/f*" coefficient curves for the 3 strategies and a constant torque

Then the efficiency maps have been subtracted:

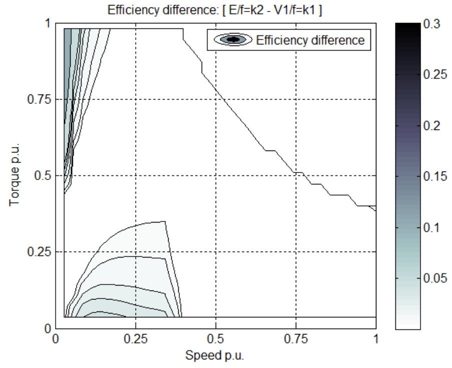

Fig. 11. Efficiency map comparison: [“*E/f=k*$_2$” map – “*V*$_1$*/f=k*$_1$” map]

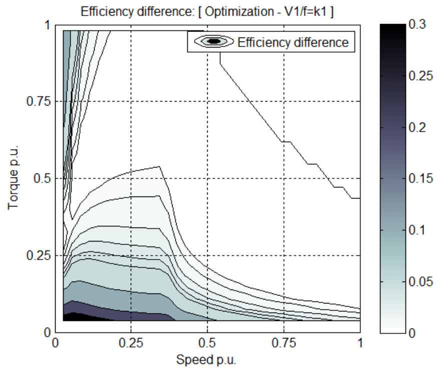

Fig. 12. Efficiency map comparison: [Optimization map – “*V*$_1$*/f=k*$_1$” map]

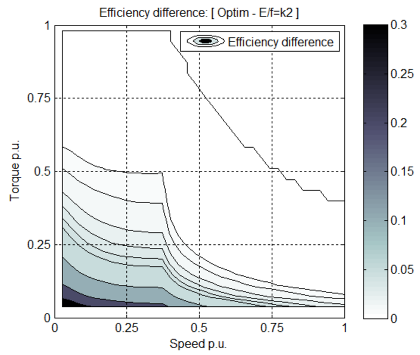

Fig. 13. Efficiency map comparison: [Optimization map – “*E/f=k*$_2$” map]

In term of efficiency, differences are mainly located at the small torque/speed operating points, where power is low and doesn’t have a strong impact on energy consumption. To assess this influence, the following plots show an electrical power comparison:

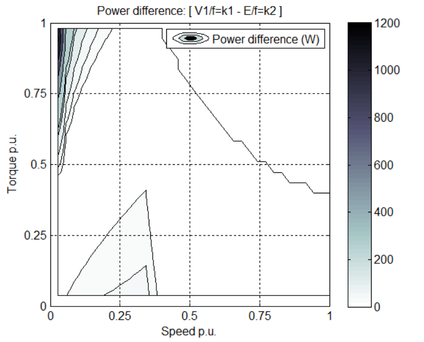

Fig. 14. Power map comparison: [“*E/f=k2*” map – “*V*$_1$*/f=k*$_1$” map]

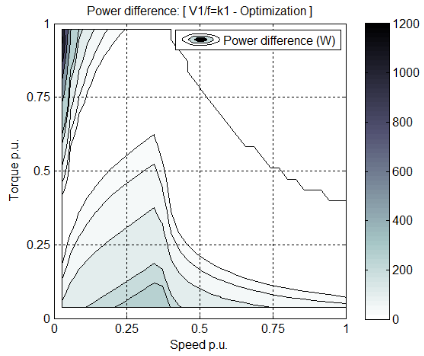

Fig. 15. Power map comparison: [Optimization map – “*V*$_1$*/f=k*$_1$” map]

Differences in term of energy consumption will only be observed if the driving cycle has operating points in the low speed/torque area. The high torque/low speed area is only for specific situations such as starting the vehicle in a slope. The differences may not have influence for driving cycle without slope.

B. Driving cycle

In order to evaluate energy consumption, the WLTC (Worldwide harmonized Light vehicles Test Procedures) driving cycle has been chosen. This cycle has been created to define a global standard for energy consumption estimation from light duty vehicles. It is divided in three class depending on power-weight ratio. Passenger cars are generally in class 3: power (W)/weight (kg) > 34. The WLTC class 3 driving cycle is itself divided in 4 parts: low, mid, high, very high. For our study, WLTC low and mid will be tested.

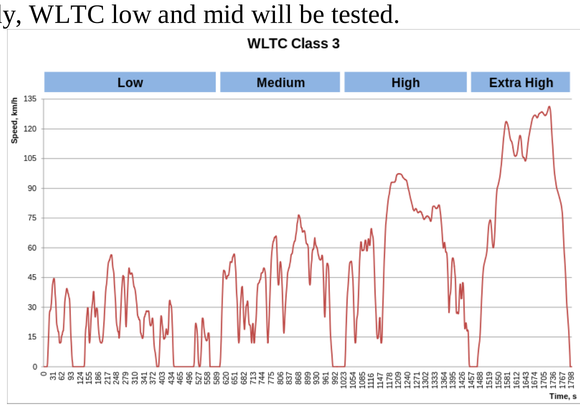

Fig. 16. WLTC driving cycle for class 3 vehicles

WLTC operating points for positive torque request have been plotted on top of the previous power comparison for our study case to evaluate their influence on the consumed energy.

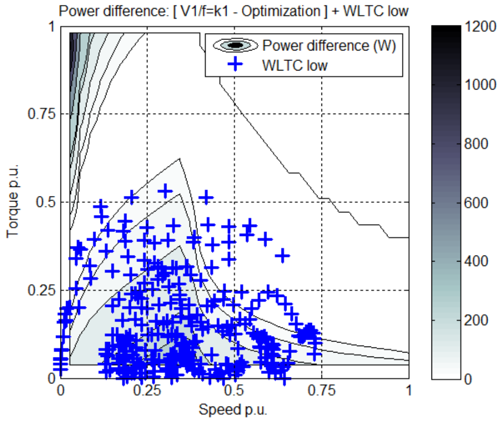

Fig. 17. Power comparison + WLTC low operating points

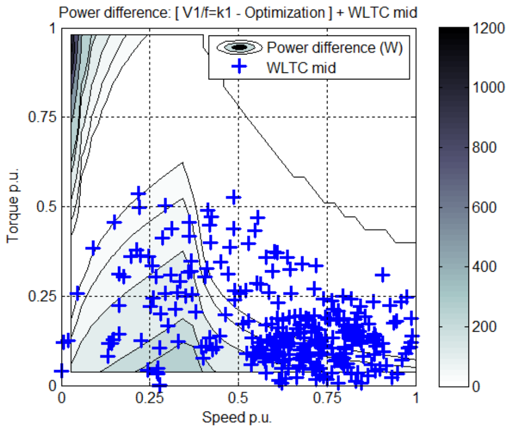

Fig. 18. Power comparison + WLTC mid operating points

WLTC low operating points are concentrated in the area with the more differences. Then the energy consumption is compared in the following table. WLTC Low with "$V_1/f=k_1$" method is taken as the reference for the comparison.

TABLE II. ENERGY CONSUMPTION IN %

Method	*WLTC Low*	*WLTC mid*
"$V_1/f=k_1$"	100%	120.8%
"$E/f=k_2$"	99.1%	120.5%
Optimization	88.1%	118.3%

The gain with optimization procedure is ~12% for WLTC low driving cycle which is not negligible and may influence the geometry sizing if included in a design optimization loop.

V. CONCLUSION

Optimizing induction machine control strategy allows to obtain significant improvements on efficiency and energy consumption of EV powertrains. The paper shows the influence of an optimized control strategy compared to a classic "V/f" method. The next step is to introduce the optimized control in a larger design optimization loop, integrating motor geometry and other powertrain elements.

ACKNOWLEDGMENT

This work is supported by RENAULT Company. The authors thank L2EP and RENAULT teams.

REFERENCES

[1] N. Janiaud, F. Vallet, M. Petit, and G. Sandou, "Electric Vehicle Powertrain Architecture and Control Global Optimization," *World Electric vehicule Journal*, vol. 3, pp. 1–12, 2009.

[2] C. Kral, A. Haumer, H. Kapeller, and F. Pirker, "Design and Thermal Simulation of Induction Machines for Traction in Electric and Hybrid Electric Vehicles," vol. 1, pp. 190–196, 2007.

[3] S. Huang, J. Luo, S. Member, F. Leonardi, and A. Member, "A General Approach to Sizing and Power Density Equations for Comparison of Electrical Machines," vol. 34, no. 1, pp. 92–97, 1998.

[4] F. W. I. Member and E. S. De Carvalho, "The Concept of Imaginary Machines for Design and Setting of Optimization Problems : Application to a Synchronous Generator," vol. 1, no. Im, pp. 1461–1466, 2012.

[5] H. Rehman and L. Xu, "Alternative Energy Vehicles Drive System: Control, Flux and Torque Estimation, and Efficiency Optimization," *IEEE Transactions on Vehicular Technology*, vol. 60, no. 8, pp. 3625–3634, Oct. 2011.

[6] C. Thanga Raj, S. P. Srivastava, and P. Agarwal, "Energy Efficient Control of Three-Phase Induction Motor - A Review," *International Journal of Computer and Electrical Engineering*, vol. 1, no. 1, pp. 61–70, 2009.

[7] F. Abrahamsen, F. Blaabjerg, J. K. Pedersen, and P. B. Thoegersen, "Efficiency-Optimized Control of Medium-Size Induction Motor Drives," *IEEE Transactions on industry applications*, vol. 37, no. 6, pp. 1761–1767, 2001.

[8] S. Chen and S.-N. Yeh, "Optimal efficiency analysis of induction motors fed by variable-voltage and variable-frequency source," *IEEE Transactions on Energy*, vol. 7, no. 3, pp. 537–543, 1992.

[9] S. M. Muyeen, *Wind Energy Conversion Systems*. Springer, 2012, p. 531.

[10] I. Boldea, L. N. Tutelea, and S. State, *Electric Machines: Steady State, Transients, and Design with MATLAB*. Taylor & Francis, 2009, p. 800.

[11] J. Pyrhonen, T. Jokinen, and V. Hrabovcova, *Design of Rotating Electrical Machines*. Wiley, 2009, p. 512.

[12] I. Kioskeridis and N. Margaris, "Loss Minimization in Induction Motor Adjustable-Speed Drives," *IEEE Transactions on industrial electronics*, vol. 43, no. 1, pp. 226–231, 1996.

[13] S. Vakkas Ustun and M. Demirtas, "Modeling and control of V / f controlled induction motor using genetic-ANFIS algorithm," *Energy Conversion and Management*, vol. 50, no. 3, pp. 786–791, 2009.

[14] V. Mester, F. Gillon, S. Brisset, and P. Brochet, "Global Optimal Design of a Wheel Traction Motor by a Systemic Approach of the Electric Drive Train," in *Vehicle Power and Propulsion Conference, 2006. VPPC '06. IEEE*, 2006, p. 6.